Carbohydrate Polymers 116 (2015) 167–172

Contents lists available at ScienceDirect

Carbohydrate Polymers

journal homepage: www.elsevier.com/locate/carbpol

Study of the chemical stability of the capsular polysaccharide produced by *Haemophilus influenzae* type b

Felipe de Oliveira Cintra, Mickie Takagi*

Laboratório de Desenvolvimento de Processos, Centro de Biotecnologia, Instituto Butantan, Brazil

ARTICLE INFO

Article history:
Received 31 December 2013
Received in revised form 13 March 2014
Accepted 3 April 2014
Available online 13 April 2014

Keywords:
PRP
Haemophilus influenzae type b
Alkaline transesterification
Polysaccharide depolymerization
Vaccine

ABSTRACT

Haemophilus influenzae type b (Hib) is a human pathogen that causes severe infections such as pneumonia, sepsis and meningitis. Vaccines for Hib infections are based on its capsular polysaccharide conjugated to a protein. This conjugated Hib antigen is included as one of the components of polyvalent vaccines and accounts for more than 50% of the total cost of the formulations. The instability of the polysaccharide is responsible for the high cost of the vaccine. In this study, the factors affecting the spontaneous degradation of the polysaccharide from Hib were evaluated based on the decrease in its molecular mass, as measured by size-exclusion chromatography. Temperature and pH were found to be the most significant variables, and the results showed that the conditions of bacterial cell growth (37 °C and pH 7.5) are favourable for depolymerization. An increase in the concentration of sodium ions up to 200 mM intensified the effect of pH, allowing higher rates of depolymerization at lower pH values, whereas the presence of magnesium ions showed no effects.

1. Introduction

Haemophilus influenzae type b (Hib) is a human pathogen associated with various health complications such as pneumonia, sepsis and meningitis, mainly in children under two years of age and immunocompromised individuals (Wilfert, 1990). Vaccination against Hib was introduced in 1987 in North America and, in the rest of the developed world in the 1990s and is currently being extended to developing countries by international organizations, such as the Global Alliance for Vaccine Innovation (GAVI) and the United Nations Children's Fund (UNICEF) (Bisgard et al., 1998; GAVI, 2013; WHO, 2013). Today, the World Health Organization (WHO) recommends the use of polyvalent formulations, which combine the Hib antigen with the Diphteria–Tetanus–Pertussis (DTP) vaccine (tetravalent) or both DTP and Hepatitis B (HepB) vaccines (pentavalent). However, the inclusion of the Hib antigen increases the cost of the polyvalent vaccines, in fact, it; represent more than half of the overall cost per dose of the formulation (UNICEF, 2013).

One of the major factors contributing to the high cost of the Hib vaccine is the inherent instability of the polysaccharide molecule. It has been demonstrated that the polysaccharide molecule of Hib undergoes spontaneous degradation under certain ambient conditions, and a molecular mass decrease has been observed during the cell growth steps (Egan, Schneerson, Werner, & Zon, 1982; Sturgess et al., 1999). The instability and consequent molecular mass decrease of the polymer has great significance on the final global productivity of the vaccine because many steps of the most recent purification and conjugation processes are based on ultrafiltration (Albani, da Silva, Takagi, & Cabrera-Crespo, 2012; Takagi et al., 2008).

The Hib vaccine is composed of a polysaccharide-protein conjugate, and the polysaccharide is the molecule present in the extracellular capsule of the bacterium. The capsular polysaccharide of Hib is formed by units of ribosyl-ribitol, that are linked together by a phosphodiester linkage, denominated poly-ribosyl-ribitol-phosphate, PRP (Egan et al., 1982).

The chemical structure of PRP is responsible for its natural instability. As shown in Fig. 1, the PRP molecule is structurally similar to the molecule of RNA: the hydroxyl at the carbon 2 of ribose is located in the proximity of the phosphate group, and in the presence of free hydroxyls in the milieu this carbon undergoes transesterification and consequent depolymerization (Egan et al., 1982). In the case of RNA, this reaction is not only affected by the concentration of hydroxyls, but also by the presence of mono and divalent metal ions, such as potassium and magnesium, which are capable of stabilizing the reactive form of the hydroxyl from ribose by reducing its pKa of ionization, by facilitating proton transfer or by acting as a Lewis acid catalyst (Li & Breaker, 1999).

Through their analysis of the PRP molecule, Egan et al. (1982) demonstrated that ions of sodium and calcium do not become strongly associated with the polysaccharide chain, even though the

* Corresponding author at: Av Vital Brasil, 1500, Butantã, CEP 05503-900, São Paulo, SP, Brazil. Tel.: +55 11 2726 9720.
E-mail address: mickie.takagi@butantan.gov.br (M. Takagi).

http://dx.doi.org/10.1016/j.carbpol.2014.04.004
0144-8617/

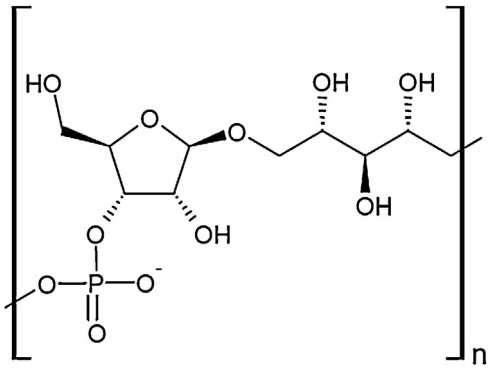

Fig. 1. Chemical structure of the poly-ribosyl-ribitol-phosphate repetitive unit.

divalent cation is indeed capable of catalysing the transesterification reaction and the monovalent cation has a significant effect on the rate of depolymerization.

The study of the depolymerization rate of PRP as functions of ambient conditions, such as pH, temperature, and ions concentrations, is of great importance to the search for vaccine production processes that are less expensive and economically viable. During all stages of production, i.e., cell growth, purification and chemical conjugation, the molecule is exposed to specific conditions that may promote chain cleavage. In the PRP production process, cell growth is conducted at a mildly alkaline pH of 7.5 (Takagi, Cabrera-Crespo, Zangirolami, Raw, & Tanizaki, 2006), demanding the addition of sodium hydroxide for pH control and thus increasing the concentration of monovalent cations. In the purification step, proteolytic enzymes and endonucleases are used for the removal of proteins and nucleic acids, and this reaction is conducted in the presence of magnesium ions at higher pH values (Albani et al., 2012).

Under these premises, this work proposes the study and quantification of the depolymerization rate of PRP by the measurement of molecular mass decrease, regarding the effects of pH, temperature and, sodium and magnesium cations concentration.

2. Materials and methods

2.1. Preparation of PRP

Strain GB3291 of *H. influenzae* type b was purchased from Instituto Adolpho Lutz (São Paulo, Brazil). The cells were cultivated in 15 L of the Modified Medium Peptone (MMP) described by Takagi et al. (2006) in a BioFlo 5000 bioreactor (New Brunswick Scientific Co., USA), until all of the glucose was consumed, as measured using at Bioliquid glicose colorimetric enzymatic kit (Laborclin LTDA, Brazil). At this point, the feeding of a concentrated solution of glucose and yeast extract (20% each) at a constant flow rate of 1.2 L h^{-1} was initiation, and this feeding was ended when the total volume in the reactor reached 60 L. Throughout the cultivation, the pH was controlled at 7.50 with 5 M NaOH, the temperature was maintained at 37 °C, the air flow rate was controlled at 15 L min^{-1}, and the dissolved oxygen was maintained at 30% of the saturation by controlling the agitation speed, which ranged from 100 to 500 rpm. The cells were separated from the culture broth in a continuous tubular centrifuge with automatic piston discharge (APD75 Celeros Inc, USA) at 20,000 g and 4 °C with a feed flow rate of approximately 200 mL min^{-1}. The isolation of PRP from the supernatant was performed by a series of diafiltrations on 100 kDa cut-off membranes, ethanol precipitations and enzymatic hydrolysis, as described by Albani et al. (2012). The final purified PRP was lyophilized and stored at −20 °C until use.

Table 1
Values of the variables at different levels in the 2^4 RCCD for the analysis of PRP stability.

Variables	Levels				
	−2	−1	0	1	2
NaCl (mM)	0	50	100	150	200
$MgCl_2$ (mM)	0	0.75	1.50	2.25	3.00
pH	5.00	5.75	6.50	7.25	8.00
T (°C)	25.00	28.75	32.50	36.25	40.00

2.2. Experimental design

A rotational central composite design (RCCD) was used for the study of the effects of the four variables (2^4), namely pH, temperature (T) and, the molarity of NaCl and $MgCl_2$ according to Table 1. The central point was performed in duplicate. The experiments were analysed using the STATISTICA® 11 software.

2.3. Measurement of PRP depolymerization rate

The solutions of PRP were prepared to obtain a concentration of 1000 mg L^{-1} and incubated in a water bath at the conditions specified by the experimental design. Samples were collected over time for the measurement of the number average molecular mass (M_n). The M_n was measured by high-performance size exclusion chromatography (HPSEC) using two serially connected 30 cm TKS Gel GMPWxl columns (TOSOH Bioscience, Japan). The chromatography was performed on a Shimadzu HPLC system, composed of an isocratic pump (10ADVp), a column oven (CTO-10ASvp), an autosampler (SIL-10ADvp), a refraction index (RI) detector (RID-10A), a system control unit (SCL-10AVp) and the Class VP version 6.2 software for data acquisition (Shimadzu Corp., Japan). A frequency of 2 Hz was used for the collection of the elution data. The mobile phase consisted of a solution of 150 mM NaCl, 10 mM Na_2HPO_4, and 0,02% NaN_3, pH of which was adjusted to 7.50 using 6 M HCl; this solution was pumped at a rate of 0.6 mL min^{-1}, and the temperature of the column and the detector cell were maintained at 40 °C. The injection volume of all of the samples was 50 μL. Under these parameters, the exclusion volume/time of the system was determined to be 21.85 min or 13.11 mL with Blue Dextran (Fluka Analytical, Sweden), whereas the total permeation volume/time was determined to be 35.00 min or 21 mL with dextrose; both reagents were prepared at a concentration of 1 g L^{-1}. The elution time of the polysaccharide was converted into values of molecular mass through a linear correlation between the elution times of low-dispersity dextrans and the logarithm of their known molecular mass; six dextran standards with nominal molecular mass (M_p) values of 1.5, 6, 10, 40, 70 and 229 kDa were used (Fluka Analytical, Sweden). The data were then used to calculate the number average molecular mass (M_n) using Eq. (1) and the mass average molecular mass (M_w) using Eq. (2), where h_i is the height of the chromatographic signal and M_i is the molecular mass value relative to the elution time of fraction i (Meunier, 1997). The ratio between the two averages, M_w/M_n, was defined as the dispersity $Đ$ of the distribution (Stepto, 2009).

$$M_n = \frac{\sum h_i}{\sum h_i/M_i} \quad (1)$$

$$M_w = \frac{\sum h_i M_i}{\sum h_i} \quad (2)$$

For the estimation of the rate of depolymerization, a linear curve was fitted to the plot of the inverse of the M_n values as a function of time. Based on the theory of random scission of polymers, the angular coefficient of this curve is proportional to the rate of

Table 2
Real and codified values of the variables studied in the 2^4 RCCD.

Assay	Real values				Codified values				Depolymerization rate ($\times 10^{-6}$ h^{-1})
	Na^+ (mM)	Mg^{2+} (mM)	pH	T (°C)	Na^+	Mg^{2+}	pH	T (°C)	
1	150	2.25	6.88	36.25	1	1	0.75	1	6.291
2	150	2.25	6.88	28.75	1	1	0.75	−1	0.950
3	150	2.25	5.66	36.25	1	1	−1.53	1	1.965
4	150	2.25	5.66	28.75	1	1	−1.53	−1	0.000
5	150	0.75	6.91	36.25	1	−1	0.80	1	5.167
6	150	0.75	6.91	28.75	1	−1	0.80	−1	0.970
7	150	0.75	5.65	36.25	1	−1	−1.55	1	1.360
8	150	0.75	5.65	28.75	1	−1	−1.55	−1	0.000
9	50	2.25	7.03	36.25	−1	1	1.03	1	6.036
10	50	2.25	7.03	28.75	−1	1	1.03	−1	1.224
11	50	2.25	5.76	36.25	−1	1	−1.35	1	1.326
12	50	2.25	5.76	28.75	−1	1	−1.35	−1	0.000
13	50	0.75	7.07	36.25	−1	−1	1.10	1	4.521
14	50	0.75	7.07	28.75	−1	−1	1.10	−1	1.600
15	50	0.75	5.82	36.25	−1	−1	−1.23	1	1.766
16	50	0.75	5.82	28.75	−1	−1	−1.23	−1	0.217
17	200	1.5	6.18	32.5	2	0	−0.56	0	0.273
18	100	3	6.27	32.5	0	2	−0.39	0	0.437
19	100	1.5	7.55	32.5	0	0	2.00	0	10.607
20	100	1.5	6.3	40	0	0	−0.34	2	3.782
21	0	1.5	6.55	32.5	−2	0	0.13	0	0.282
22	100	0	6.33	32.5	0	−2	−0.28	0	0.127
23	100	1.5	5.41	32.5	0	0	−2.00	0	0.453
24	100	1.5	6.29	25	0	0	−0.36	−2	0.171
25	100	1.5	6.28	32.5	0	0	−0.37	0	0.000
26	100	1.5	6.28	32.5	0	0	−0.37	0	0.000

polymerization, as visualized from Eq. (3), where M_{n0} is the value of M_n at the start of the experiment, k is the rate of the depolymerizing reaction, and m_0 is the molecular mass of the repetitive unit of the polymer (Bradley & Mitchell, 1988). In the case of PRP, m_0 is the molecular mass of the ribosyl-ribitol-phosphate unit and is equal to 345.22 Da.

$$\frac{1}{M_n} = \frac{1}{M_{n0}} + \frac{k}{2m_0}t \quad (3)$$

3. Results and discussion

The capsular polysaccharide from Hib, PRP, was produced through a fed-batch process and purified by ultrafiltration technology, ethanol precipitation and enzymatic hydrolysis with an overall recovery ratio of approximately 23% in terms of polysaccharide. For the molecular mass characterization of this polysaccharide, the necessary calibrations of the size-exclusion column were made using standard dextrans. The elution profile of six dextran standards is illustrated in Fig. 2A; the correlation of the elution time and the logarithm of the molecular weight of the standards is shown to be linear in Fig. 2B; and was used to determine the relative molecular weight of our samples.

The purified PRP was characterized as having an initial number average molecular mass of approximately 275 kDa, with a dispersity value not greater than 1.45. The lyophilized polysaccharide was solubilized in solutions of known pH, which was controlled with equimolar solutions of Na_2HPO_4 and NaH_2PO_4 (10 mM), and with known NaCl and $MgCl_2$ molarities. A total of 26 solutions were prepared, according to the variations proposed by the 2^4 RCCD. However, the solubilization of the lyophilized PRP had the effect of altering the pH of the solution, despite the presence of the phosphate buffer. This behaviour was observed due to presence of a phosphate group in the PRP molecule, which may change the ionization of the free phosphate groups. Therefore, the real pH values of the prepared solutions were directly measured, and the values were then rescaled into the codified values under the range from −2 to +2. Table 2 shows the final configuration of the experimental design, with the real pH values and the four codified variables.

Each of the 26 solutions were incubated at the determined temperature and sampled at progressive time intervals. The M_n was immediately measured, and the curve of $1/M_n$ was used to estimate the rate of transesterification of the phosphodiester linkage. This rate is also shown in Table 2, for each of the conditions tested. A quadratic model was considered for each of the four variables tested, and one-by-one interactions between them were also considered. The coefficients were tested for statistical significance by taking the standard error from the linear regression and building a t statistic. A level of significance of 0.05 was initially considered to account for significant effects. The effects considered significant and their statistics are listed in Table 3.

The global quadratic model, which accounted for four linear effects, four quadratic effects, six interactions and one intercept, had many insignificant variables. These were removed one by one, starting from the least significant, i.e., from the one with the smallest absolute value for the t statistic. Through this process the model can be reduced to a simpler model in which all of the coefficients with the exception of one were under the level of significance. As detailed in Table 2, the coefficient related to the effect of Na^+ molarity in this simplified model has a p-value of 0.082, which is above the level of significance. Although, we observed that the removal of this coefficient decreased the overall quality of the model. In fact,

Table 3
Coefficients and statistical significance of the factors considered for PRP depolymerization.

Factor	Coefficient	Error	t statistic (18)	p-Value
$[Na^+]$ (Linear)	4.30E−07	2.34E−07	1.84	0.082
pH (linear)	2.78E−06	2.10E−07	13.19	<0.001
T (linear)	2.08E−06	2.34E−07	8.90	<0.001
$[Na^+]$ vs. pH	4.98E−07	2.36E-07	2.11	0.049
pH vs. T	8.37E−07	2.34E−07	3.58	0.002
pH (quadratic)	1.81E−06	2.09E−07	8.69	<0.001
T (quadratic)	6.44E−07	2.22E−07	2.91	0.009

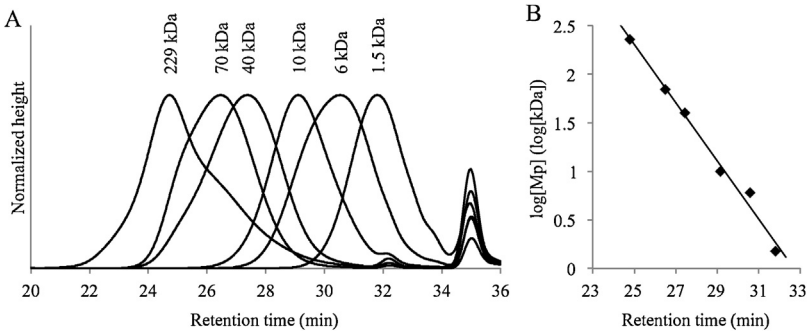

Fig. 2. (A) HPSEC-RI elution profiles of the dextran standards. The peak at 35 min is related to the salts in the sample buffer that eluted at the total permeation volume. (B) Linear correlation between the retention times and the logarithm of the molecular weights of the dextran standards.

the removal of this coefficient increased the *p*-value of the interaction between the molarity of Na and pH from 0.049 to 0.121, thereby considerably surpassing the level of significance. Additionally, both the normality of the residuals and the adjusted coefficient of correlation decreased. Based on this scenario, we chose to tolerate a higher level of significance for the model to include the effect of the molarity of Na^+. Therefore, the experimental data may provide detailed insights into the factors that contribute to PRP depolymerization. The pH, temperature (*T*) and molarity of Na^+ were characterized as significant, whereas the molarity of Mg^{2+} did not appear to have an effect.

The most significant variables, namely the pH and temperature, were expected to show significance. Fig. 3 shows the response surface for these two variables, at a constant Na^+ molarity of 100 mM. Over the range of values studied, it becomes clear that the depolymerization rate is increased at pH values over neutrality; and always increases with increases in temperature. At more acidic pH values, e.g., at pH values less than 6.5, depolymerization is virtually non-existent. The quadratic model does predict an increase in the rate of reaction in the acidic direction, although it may be argued that it represents a lack of fit in this region because experimental values are not available.

The effect of Na^+ molarity can be visualized through its interaction with pH, as shown in Fig. 4. The presence of these monovalent ions shift the response surface toward the acidic region. The analysis of the lines at a given pH shows, that an increase the concentration of sodium ions increases the rate of depolymerization, i.e., the monovalent cation increases the action of the hydroxyls in the alkaline catalysis process. This finding is consistent with a previous description of the action of potassium cations on the rate of transesterification of RNA. A monovalent ion may act by stabilizing the reactive form of the hydroxyl at carbon 2 from ribose, and by reducing the pKa of ionization of this group (Li & Breaker, 1999).

The effect of Mg^{2+} molarity, despite being well characterized for the depolymerization of RNA, showed no statistical significance in this experiment. In the study reported by Li and Breaker (1999), the effect of this cation was assayed at higher pH values, in the range from 8.5 to 10.0. At lower pH values, i.e., in the range studied here, the effect may be not observable. Furthermore, Egan et al. (1982) reported that divalent calcium ions do not associate intimately with PRP, which is contrary to what is observed for other polyelectrolytes, and this finding may also be true for magnesium. These researchers also reported that the presence of sodium reduces the catalytic activity of calcium. In a study of RNA depolymerization, Li and Breaker (1999) also observed a reduction in the catalytic activity of magnesium due to the presence of potassium and therefore; argued that the monovalent ion may shield the phosphate group from association with the divalent ion. In our experimental design, no experiment was conducted with the presence of magnesium alone, i.e., in the absence of sodium. Thus, we may suggest that the catalytic activity of magnesium on the depolymerization of PRP was not observed due to both the presence of sodium cations and the low range of pH values studied.

The characterization of the main factors that contribute to depolymerization and the quantification of the rates of reaction as functions of these factors are important for the optimization and cost minimization of Hib vaccine production. In the upstream process, cell growth has limited productivity due to the

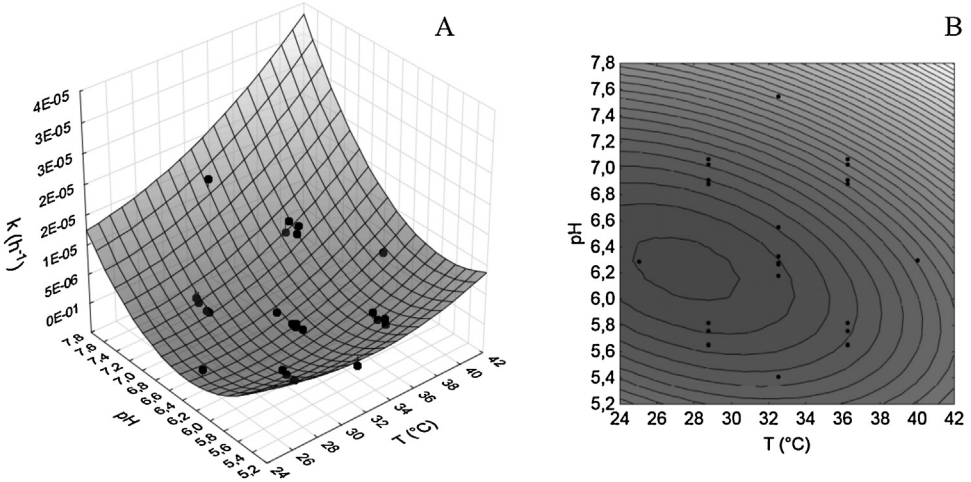

Fig. 3. 3D plot (A) and contour plot (B) of the response surface of the effects of pH and temperature on the rate of PRP degradation, at a fixed NaCl concentration of 100 mM.

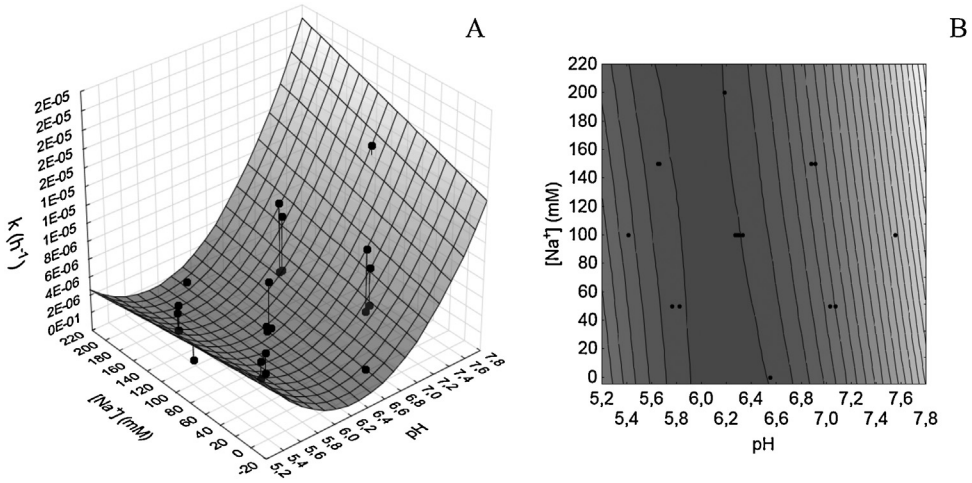

Fig. 4. 3D plot (A) and contour plot (B) of the response surface of the effects of pH and NaCl on the rate of PRP degradation, at a fixed temperature of 32.5 °C.

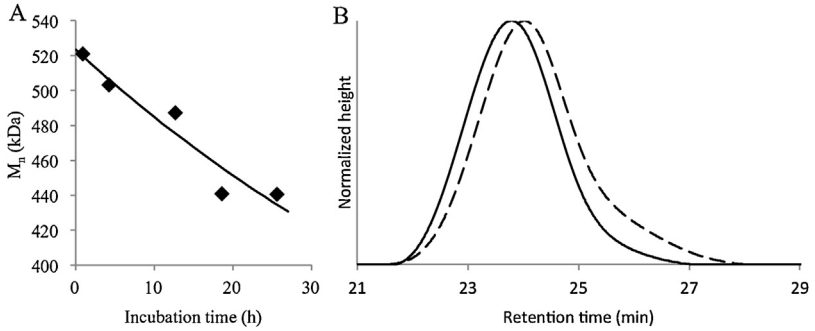

Fig. 5. (A) Measurement and simulation of the decrease in the PRP molecular mass under the pH and temperature conditions used for cell growth. (B) HPSEC-RI elution profiles of the PRP before and after 25 h of incubation: the continuous line: represents the sample at the beginning of the experiment, and the; dashed line: corresponds to the sample at the end of the experiment.

fastidious nature of the bacterium's metabolic network, which limits the total PRP formation. The processes described in the literature for this step cite the use of mildly alkaline pH values, such as 7.30 and 7.50, the use of physiological temperatures (36–37 °C) and the addition, of large quantities of NaOH (up to 900 mM in the final broth) during the cell growth for the control of the pH (Merritt, Allard, O'Toole, Swartz, & Licari, 2000; Takagi et al., 2006). Based on the results of this study, it is clear that these conditions are unfavourable for the stability of the PRP molecule. The ongoing depolymerization of PRP during cell growth shall result in a final product with a low molecular mass, which directly affects the purification process based on ultrafiltration technology. In our laboratory, we observed that long fed-batch cultivations resulted in a final PRP molecule with a molecule weight of less than 300 kDa (data not shown).

To illustrate the severity of this issue, the conditions of cell growth reported by Takagi et al. (2006) (pH 7.50, 37 °C and 150 mM NaCl) were replicated. A different sample of purified PRP, with a starting M_n value of 521 kDa and a $Đ$ value of 1.31, was incubated under these conditions using the same protocol that used for the experimental design. As shown in Fig. 5A, a decrease in the molecular mass was observed, which simulates the phenomenon that occurs in the bioreactor. During a period of 24 h, which is a reasonable duration of a fed-batch process, the molecular mass was observed to decrease by approximately 16% with an overall depolymerization rate of $1.054 \times 10^{-5}\ h^{-1}$, as calculated using Eq. (3). Fig. 5B illustrates the elution profile of this sample at the beginning and end of the depolymerization reaction. As shown, it is possible to observe that the depolymerization process is responsible for shifting the whole distribution toward an increased retention time and; thus a lower molecular mass. It is also possible to observe increases in the fraction of smaller molecules in the population and its dispersity, which showed a value of 1.36 at the end of the assay.

4. Conclusion

By introducing an ultrafiltration-based PRP purification process, Albani et al. (2012), observed that low recovery ratios, (in the order of less than 25%), are correlated with the duration of the cell growth step. These researchers used, a long fed-batch process, which resulted in the production of a relatively high quantity of PRP. However approximately half of the material was lost during the first ultrafiltration step. As quantified in this work is explained by the inherent instability of the molecule; associated with the cultivation conditions used. In addition, this instability is responsible for shifting the whole distribution of the polysaccharide toward a lower molecular mass and for increasing the fraction of smaller molecules in the population, which can be easily lost in ultrafiltration processes. In conclusion, we conclude that the conditions used during cell growth, mainly pH and temperature, must be changed to avoid the spontaneous degradation observed. Similarly, the conditions used for the purification process should also be adapted based on the influence of pH, temperature, and sodium ions on PRP stability to achieve higher recovery ratios in the downstream processes.

Acknowledgments

We gratefully acknowledge the financial support provided by the Butantan Foundation and BNDES (N° 11.2.0322.1/2012). We also thank Mr. Lourivaldo Inácio de Souza and Ms Ana Maria Soares Rodrigues for the technical assistance.

Appendix A. Supplementary data

Supplementary material related to this article can be found, in the online version, at http://dx.doi.org/10.1016/j.carbpol.2014.04.004.

References

Albani, S. M. F., da Silva, M. R., Takagi, M., & Cabrera-Crespo, J. (2012). Improvement in the purification process of the capsular polysaccharide from *Haemophilus influenzae* type b by using tangential ultrafiltration and diafiltration. *Applied Biochemistry and Biotechnology*, *167*(7), 2068–2075.

Bisgard, K. M., Kao, A., Leake, J., Strebel, P. M., Perkins, B. a., & Wharton, M. (1998). *Haemophilus influenzae* invasive disease in the United States, 1994–1995: Near disappearance of a vaccine-preventable childhood disease. *Emerging Infectious Diseases*, *4*(2), 229–237.

Bradley, T. D., & Mitchell, J. R. (1988). The determination of the kinetics of polysaccharide thermal degradation using high temperature viscosity measurements. *Carbohydrate Polymers*, *9*(4), 257–267.

Egan, W., Schneerson, R., Werner, K. E., & Zon, G. (1982). Structural studies and chemistry of bacterial capsular polysaccharides. Investigations of phosphodiester-linked capsular polysaccharides isolated from *Haemophilus influenzae* types a, b, c, and f: NMR spectroscopic identification and chemical modification. *Journal of the American Chemical Society*, *104*(10), 2898–2910.

GAVI. (2013). *Hib vaccine*. Retrieved from http://www.gavialliance.org/support/nvs/hib/

Li, Y., & Breaker, R. R. (1999). Kinetics of RNA degradation by specific base catalysis of transesterification involving the 2′-hydroxyl group. *Journal of the American Chemical Society*, *121*(23), 5364–5372.

Merritt, J., Allard, G., O'Toole, L., Swartz, R., & Licari, P. (2000). Development and scale-up of a fed-batch process for the production of capsular polysaccharide from *Haemophilus influenzae*. *Journal of Biotechnology*, *81*(2-3), 189–197.

Meunier, D. M. (1997). Molecular weight determinations. In F. A. Settle (Ed.), *Handbook of instrumental techniques for analytical chemistry* (pp. 853–866). Upper Saddle River: Prentice-Hall.

Stepto, R. F. T. (2009). Dispersity in polymer science (IUPAC recommendations 2009). *Pure and Applied Chemistry*, *81*(2), 351–353.

Sturgess, A. W., Rush, K., Charbonneau, R. J., Lee, J. I., West, D. J., Sitrin, R. D., et al. (1999). *Haemophilus influenzae* type b conjugate vaccine stability: Catalytic depolymerization of PRP in the presence of aluminum hydroxide. *Vaccine*, *17*(9–10), 1169–1178.

Takagi, M., Cabrera-Crespo, J., Zangirolami, T. C., Raw, I., & Tanizaki, M. M. (2006). Improved cultivation conditions for polysaccharide production by *H. influenzae* type b. *Journal of Chemical Technology & Biotechnology*, *81*(2), 182–188.

Takagi, M., Lima, R. B., Albani, S. M. F., Zangirolami, T. C., Tanizaki, M. M., & Cabrera-Crespo, J. (2008). Purification of capsular polysaccharide produced by *Haemophilus influenzae* type b through a simple, efficient and suitable method for scale-up. *Journal of Industrial Microbiology & Biotechnology*, *35*(11), 1217–1222.

UNICEF. (2013). *Vaccine Price Data*. Retrieved from http://www.unicef.org/supply/index_57476.html

WHO. (2013). *Immunization surveillance, assessment and monitoring*. Retrieved from http://www.who.int/immunization_monitoring/diseases/Hib/en/index.html

Wilfert, C. M. (1990). Epidemiology of *Haemophilus influenzae* type b infections. *Pediatrics*, *85*(4 Pt 2), 631–635.